2-DOF Helicopter Controlling by Pole-Placements

Giovanni Gallon Neto*, Fernando dos Santos Barbosa† and Bruno Augusto Angélico‡
Laboratório de Controle Aplicado - Laboratório de Automação e Controle
Departamento de Telecomunicações e Controle
Escola Politécnica da Universidade de São Paulo
*giovanni.neto@usp.br
†barbosa.fs@usp.br
‡angelico@lac.usp.br

***Abstract*— A two-degree-of-freedom (2DOF) Helicopter is an interesting way to study simple cases of multivariable systems. With existing nonlinearities and output coupling, several control methods can be implemented on this plant. The main objective of this work is to test the pole placement control technique. Therefore, the plants model development is shown using Lagrange's method followed by its linearization around small angles. Next, the controller is designed using the pole placement technique, with the use of integrators to guarantee null steady-state error. Lastly, the controller is simulated with the use of computational tools and tested on the built helicopter.**

I. Introduction

Multiple Input Multiple Output systems (MIMO) are commonly found in many practical cases in the process industry, aerospace industry, among others. In some cases there is no interaction between system variables, i.e., they are uncoupled. In other cases, there are interactions between variables, which makes the design of the controllers harder [1].

A MIMO system example is a simplified system of a helicopter with two degrees-of-freedom (2DOF) [2][3][4]. The model with two degrees of freedom is interesting because it allows the study of advanced control techniques that can be applied in real situations of flight control, behavior of rigid bodies helicopters, and aircraft. There are some commercial 2DOF helicopters plant options such as shown in [5]. However, such solutions are costly, which makes the acquisition of a dozen of them to equip a laboratory class impracticable.

Generally, multivariable control techniques for critical systems, such as aviation, are robust. For example, in [3] an adaptive robust linear quadratic regulator is proposed for application in a 2DOF helicopter. In [4], a robust optimal control using linear matrix inequalities - LMI (Linear Matrix Inequalities) with Takagi-Sugeno fuzzy controllers is considered. Another interesting control strategy of a 2DOF helicopter is the use of control technique for pole placement, which will be treated in this work.

This article begins with the development of the mathematical modeling of the system, followed by a section which consists in the construction of the prototype. Then, the implemented controller is presented, as the simulation, results and conclusion

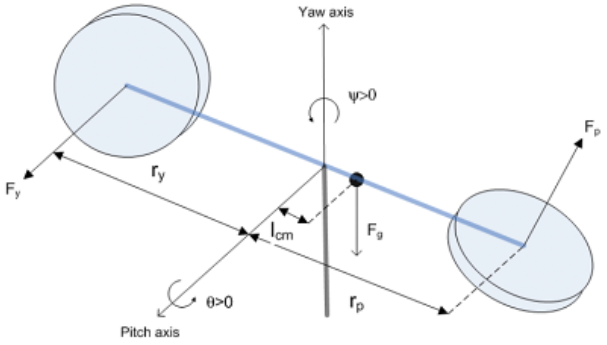

Fig. 1. Simple free-body diagram. Adapted from [5]

II. Modeling

Figure 1 presents the free-body diagram of the system used in the Lagrangian modeling process. The following convention was adopted in the modeling:

1) It rotates around two axes, pitch and yaw (θ and ψ);
2) Helicopter is horizontal with $\theta = 0$;
3) $\dot{\theta}$ is positive when the nose is moving upwards;
4) $\dot{\psi}$ is positive when the helicopter rotates clockwise;
5) There is neither rolling nor axial movements.

As stated before, this helicopter is a MIMO system with coupled response, i.e., the pitch motor controls directly the pitch angle using the force generated by its propeller, creating a torque in yaw as effect of air resistance. In order to mathematically describe the resulting torques on each axis, a good approximation commonly made is to admit that the propeller produces a force and a torque proportional to its squared speed, i.e.,

$$F = K_f \Omega^2 \quad \text{and} \quad T = K_t \Omega^2 \ . \tag{1}$$

Applying this to the helicopter, pitch and yaw resulting torques are written as

$$\tau_p = l_p K_{pp} \Omega_p^2 + K_{py} \Omega_y^2 \tag{2}$$

$$\tau_y = l_y K_{yy} \Omega_y^2 + K_{yp} \Omega_p^2 \tag{3}$$

where K_{pp} is the pitch motor thrust constant, K_{py} is the yaw motor torque constant, K_{yp} is the pitch motor torque constant, K_{yy} is the yaw motor thrust constant, Ω_p^2 is the pitch motor squared speed, Ω_y^2 is the yaw motor squared speed and l_p and

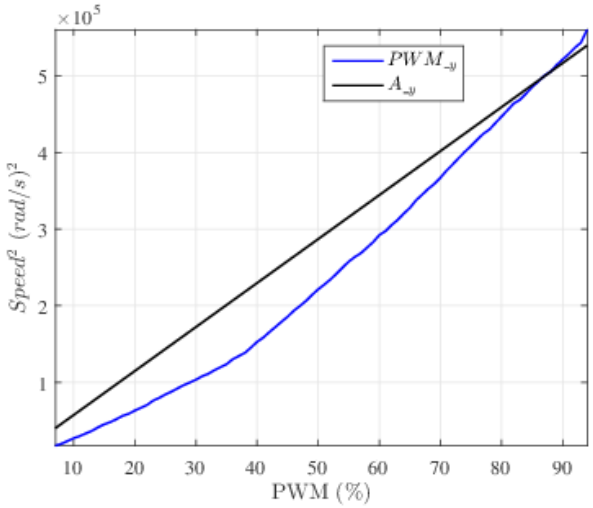

Fig. 2. Linear approximation of the motor squared speed, with $R^2 = 0.971$.

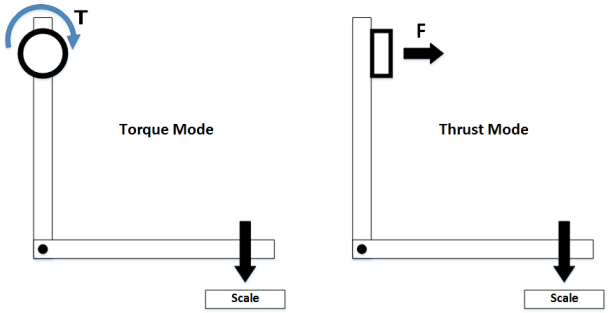

Fig. 3. Test bench to get the torque, thrust and rotational speed parameters for each motor

l_y are, respectively, the distance of each motor to the center of rotation of the helicopter.

Using a equipment such as shown in Figure 3, some tests were made using the brushless motors used in the system. Torque, thrust and rotational speed parameters were obtained for each of the PWM levels of each brushless motor.

It was observed that the squared rotational speed could be approximated by a linear relationship with the PWM level, as can be seen in Figure 2, which correlates those results to the yaw motor. Approaching the obtained results by polynomials of first degree passing through the origin, Ap and Ay parameters were obtained, which respectively relate to pitch and yaw motors.

Solving the Euler-Lagrange's equation results in a non-linear equation of motion [6]:

$$\ddot{\theta} = \frac{l_p K_{pp} A_p PWM_p + K_{py} A_y PWM_y - \left(B_p \dot{\theta} + \alpha + \beta\right)}{J_{eq\_p} + m_{heli} l_{cm}^2} \quad (4)$$

$$\alpha = m_{heli} l_{cm}^2 \dot{\psi}^2 \sin(\theta)\cos(\theta) \quad (5)$$

$$\beta = m_{heli} g \cos(\theta) l_{cm} \quad (6)$$

$$\ddot{\psi} = \frac{l_y K_{yy} A_y PWM_y + K_{yp} A_p PWM_p + \gamma - B_y \dot{\psi}}{J_{eq\_y} + m_{heli}\cos(\theta)^2 l_{cm}^2} \quad (7)$$

$$\gamma = 2 m_{heli} l_{cm}^2 \sin(\theta)\cos(\theta)\dot{\psi}\dot{\theta}, \quad (8)$$

with m_{heli} being the helicopter total moving mass, g gravity, l_{cm} the center of mass distance to origin, B_p and B_y as the movement resistance acting above pitch and yaw axes, respectively, J_{eq_p} and J_{eq_y} are the equivalent moment of inertia related to pitch and yaw, respectively.

Linearizing the system for small angles, as this is the operating point, the equations of motion are defined by

$$\ddot{\theta} = \frac{l_p K_{pp} A_p PWM_p + K_{py} A_y PWM_y - B_p \dot{\theta} - m_{heli} g l_{cm}}{J_{eq\_p} + m_{heli} l_{cm}^2} \quad (9)$$

$$\ddot{\psi} = \frac{l_y K_{yy} A_y PWM_y + K_{yp} A_p PWM_p - B_y \dot{\psi}}{J_{eq\_y} + m_{heli} l_{cm}^2}. \quad (10)$$

A state-space system is written based on these equations, resulting in:

$$\dot{\mathbf{x}}(t) = \mathbf{A}\mathbf{x}(t) + \mathbf{B}\mathbf{u}(t) \quad (11)$$

$$\mathbf{y}(t) = \mathbf{C}\mathbf{x}(t) \quad (12)$$

where $x(t)$ corresponds to system states and $u(t)$ the motors percentage inputs, defined by

$$\mathbf{x} = \begin{bmatrix}\theta & \psi & \dot{\theta} & \dot{\psi}\end{bmatrix}^T \quad \text{and} \quad \mathbf{u} = \begin{bmatrix}PWM_p & PWM_y\end{bmatrix}^T. \quad (13)$$

The matrices A, B and C, then, are written as

$$\mathbf{A} = \begin{bmatrix} 0 & 0 & 1 & 0 \\ 0 & 0 & 0 & 1 \\ 0 & 0 & \frac{-B_p}{J_{eq\_p} + m_{heli} l_{cm}^2} & 0 \\ 0 & 0 & 0 & \frac{-B_y}{J_{eq\_y} + m_{heli} l_{cm}^2} \end{bmatrix}$$

$$\mathbf{B} = \begin{bmatrix} 0 & 0 \\ 0 & 0 \\ \frac{l_p K_{pp} A_p}{J_{eq\_p} + m_{heli} l_{cm}^2} & \frac{K_{py} A_y}{J_{eq\_p} + m_{heli} l_{cm}^2} \\ \frac{K_{yp} A_p}{J_{eq\_y} + m_{heli} l_{cm}^2} & \frac{l_y K_{yy} A_y}{J_{eq\_y} + m_{heli} l_{cm}^2} \end{bmatrix}$$

$$\mathbf{C} = \begin{bmatrix} 1 & 0 & 0 & 0 \\ 0 & 1 & 0 & 0 \end{bmatrix}.$$

A. Helicopter Parameters

The first step in building the prototype shown in Figure 4 was to design the simplified helicopter body. Searches were performed to compare proportions of commercial models and AutoCAD (AutoDesk) was used to do the necessary drawings. The prototype consists of a wooden body simulating a simplified helicopter system and a base plate. It is controlled by two brushless DC motors with 9-inch propellers.

Fixed at each axis there is an angular position transducer (encoder), responsible for measuring the variation of each angle.

As one of the factors valued by this prototype was safety, it was decided to design a protection for the propellers, which offer potential risk, due to the high speeds that they can achieve, and then preventing serious accidents when handled by an inattentive operator.

In order to measure the necessary parameters for controller design and simulation, the brushless motors were identified with hall sensor and a scale. Table I contains the system parameters, in which some were obtained by linearizing thrust and torque equations and others by simple system identification.

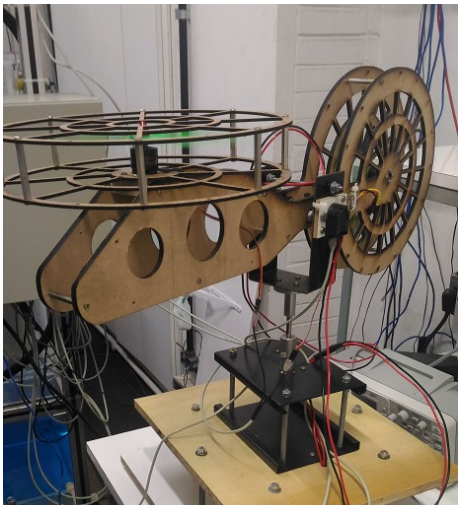

Fig. 4. 2DOF Helicopter built.

TABLE I
HELICOPTER PARAMETERS

Parameter	Value	Unit
m_{heli}	1.317	kg
l_{cm}	0.038	m
K_{pp}	$9.0131 \cdot 10^{-6}$	$N/(rad/s)^2$
K_{vy}	$-5.6680 \cdot 10^{-6}$	$N/(rad/s)^2$
K_{py}	$-1.6633 \cdot 10^{-7}$	$N.m/(rad/s)^2$
K_{yp}	$1.4887 \cdot 10^{-7}$	$N.m/(rad/s)^2$
B_p	0.1	$N/\%$
B_y	0.1	$N/\%$
J_{eq_p}	0.384	$kg.m^2$
J_{eq_q}	0.0432	$kg.m^2$
l_p	0.25	m
l_y	0.20	m
A_p	5740.2	$(rad/s)^2/\%$PWM
A_y	5741.3	$(rad/s)^2/\%$PWM
Helicopter length	0.737	m
Propeller diameter	22.86	cm
Pitch angle range	85	deg
Yaw angle range	360	deg
Pitch encoder resolution	1024	$counts/rev$
Yaw encoder resolution	1024	$counts/rev$

III. CONTROLLER DESIGN

Consider the system described by [7]

$$\dot{\mathbf{x}}(t) = \mathbf{A}\mathbf{x}(t) + \mathbf{B}\mathbf{u}(t) \quad (14)$$
$$\mathbf{y}(t) = \mathbf{C}\mathbf{x}(t) \quad (15)$$

where, for the 2DOF Helicopter:

$\mathbf{x}(t)$ is a $4x1$ state vector;
$\mathbf{y}(t)$ is a $2x1$ output vector;
$\mathbf{u}(t)$ is a $2x1$ input vector;
$\mathbf{A}, \mathbf{B}, \mathbf{C}$ matrices of appropriate size.

To get a null steady-state error, the use of integrators is considered. The input signal, as shown in Figure 5, can be described by

$$\mathbf{u}(t) = -\mathbf{K}\mathbf{x}(t) + \mathbf{K}_I\mathbf{v}(t), \quad (16)$$

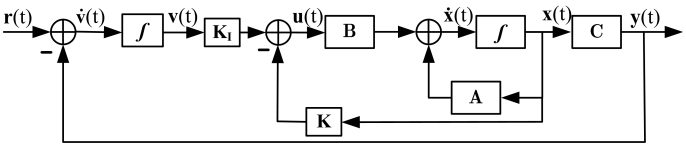

Fig. 5. Block Diagram Representation for the system.

with the integrator equation being

$$\dot{\mathbf{v}}(t) = \mathbf{r}(t) - \mathbf{y}(t) = \mathbf{r}(t) - \mathbf{C}\mathbf{x}(t). \quad (17)$$

By substituting (16) in (14), the Figure 5 closed-loop system can be described by

$$\dot{\mathbf{x}}(t) = (\mathbf{A} - \mathbf{B}\mathbf{K})\mathbf{x}(t) + \mathbf{K}_I\mathbf{v}(t), \quad (18)$$

that, along with (17), can be written in a compact way with the use of matrices:

$$\begin{bmatrix} \dot{\mathbf{x}}(t) \\ \dot{\mathbf{v}}(t) \end{bmatrix} = \begin{bmatrix} \mathbf{A} - \mathbf{B}\mathbf{K} & \mathbf{K}_I \\ -\mathbf{C} & \mathbf{0} \end{bmatrix} \begin{bmatrix} \mathbf{x}(t) \\ \mathbf{v}(t) \end{bmatrix} + \begin{bmatrix} \mathbf{0} \\ \mathbf{r}(t) \end{bmatrix}. \quad (19)$$

Using that representation, a new open-loop system can be written with the use of the following matrices:

$$\begin{aligned} \mathbf{A}_{amp} &= \begin{bmatrix} \mathbf{A} & \mathbf{0} \\ -\mathbf{C} & \mathbf{0} \end{bmatrix} \\ \mathbf{B}_{amp} &= \begin{bmatrix} \mathbf{B} \\ \mathbf{0} \end{bmatrix} \\ \mathbf{C}_{amp} &= \begin{bmatrix} \mathbf{C} & \mathbf{0} \end{bmatrix} \\ \mathbf{K}_{amp} &= \begin{bmatrix} \mathbf{K} & -\mathbf{K}_I \end{bmatrix}. \end{aligned}$$

Pole placement design [8] is used to create the matrix $\mathbf{K}_{amp}$ for the following desired closed-loop poles:

$$\mathbf{p}_{amp} = \begin{bmatrix} -6 \\ -5 \\ -2 \\ -2 \\ -0.5 \\ -0.5 \end{bmatrix}. \quad (20)$$

Using Matlab command *place*, the K_{amp} gain matrix obtained was:

$$\mathbf{K}_{amp} = \begin{bmatrix} 432.1655 & -43.2490 & 228.3272 & \dots \\ 64.8868 & -110.8425 & 33.2366 & \dots \\ \dots & -17.2390 & -160.8151 & 17.0929 \\ \dots & -43.5168 & -24.3725 & 41.5380 \end{bmatrix}. \quad (21)$$

IV. SIMULATION AND RESULTS

Using the Simulink software, the designed controller was implemented and simulated. The simulation procedures were:

- Wait for the system to stabilize at the horizontal position ($\theta = 0$ and $\psi = 0$).
- At the time of $t = 20s$, give a step signal of 0.2rad for pitch angle.
- At the time of $t = 35s$, give a step signal of -0.2rad for yaw angle.

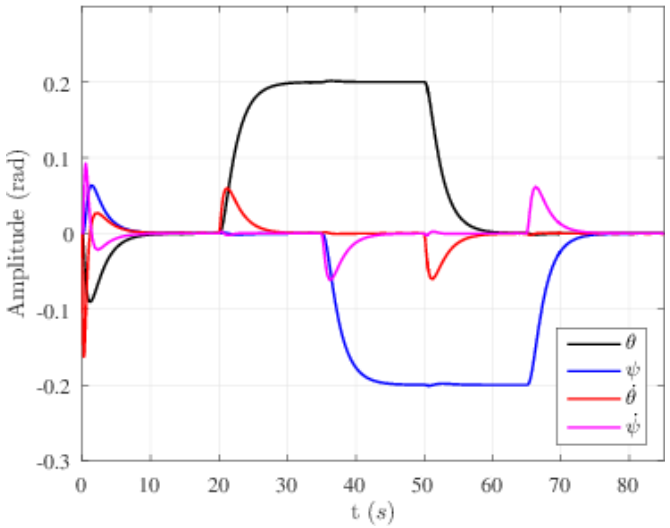

Fig. 6. Signal states used as reference.

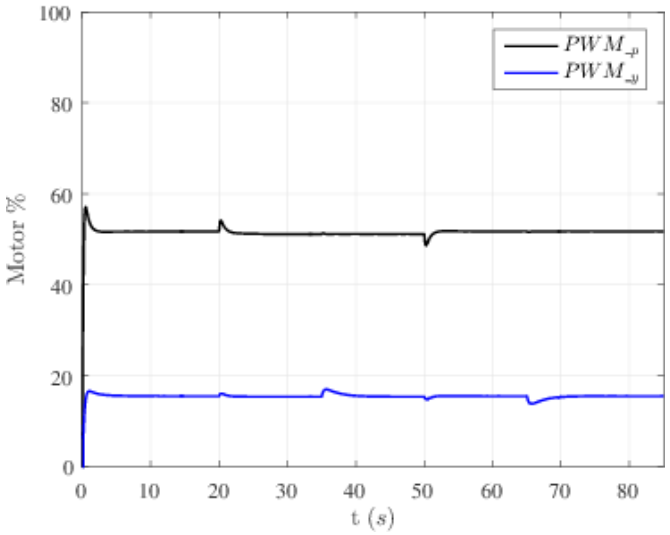

Fig. 7. Motors percentage use for the simulation

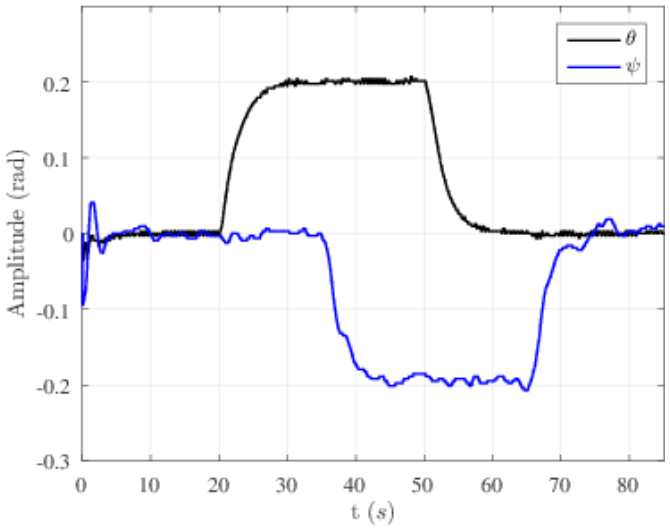

Fig. 8. Results from the controller applied to the built prototype.

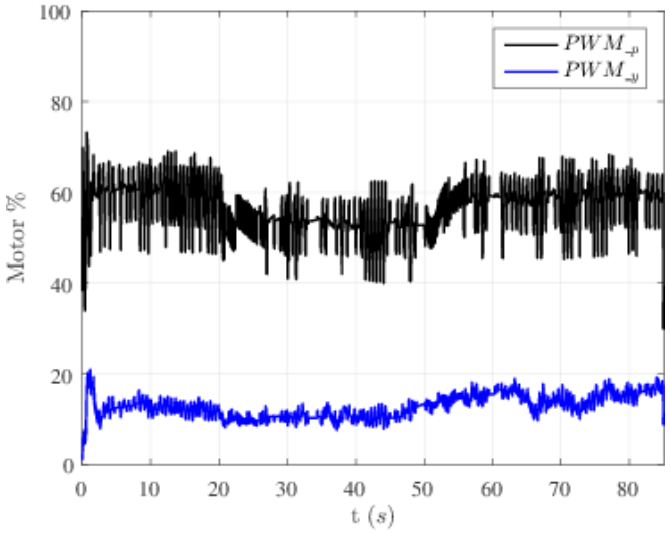

Fig. 9. Motors percentage use for the built prototype.

- At the time of $t = 50s$ give a new reference for pitch angle, bringing it back to zero, and do the same for yaw angle at the time of $t = 65s$.

Figure 6 shows all the four states and their response to the simulation procedure, proving the stabilization capability of the chosen poles. The control effort is shown in Figure 7.

The next step was uploading the controller to the development board and controlling the real helicopter. The same test procedure presented for the simulation was used. Figure 8 presents the real system response and Figure 9 shows the respective motor percentage. The main differences from the simulated system may be caused by poor system identification as well as by the power cable position, causing unmodeled dynamics.

V. Conclusion

It was shown on this work the results obtained with the implementation of a pole-placement control on a 2-DOF Helicopter. The controller designed with the use of integrator was able to stabilize the helicopter even far from the chosen operation point. Notice that when the integrator poles tend to zero, the system response to a step reference takes a longer time to reach the final value of the reference. However, there is a limit to choose those integrator poles, which will still make the system able to be controlled.

The use of integrators guaranteed zero steady-state error and it was able to follow both pitch and yaw reference steps, as shown on figure 8.

The existence of ripple in Figure 9 is generated by the measurement noise added by the encoders. Such characteristic was not included in simulation, what explains the clean control effort in Figure 7.

Future works consist in implement better system identifications, and correct existing unmodeled dynamics. The study of other controllers is also considered.

ACKNOWLEDGMENT

The authors would like to thank the Programa de Excelência Acadêmica (Proex) from the Coordination for the Improvement of Higher Education Personnel (CAPES) for grant 0212083 and the National Counsel of Technological and Scientific Development (CNPq) for grant 151881/2015-4. We also thank Kennedy X. B. Peixoto for his incredible work and help with building the helicopter and Freescale for donating the FRDM-K64F development platforms.

REFERENCES

[1] Q.-G. Wang, *Decoupling Control*, 1st ed., ser. Lecture Notes in Control and Information Sciences. Springer-Verlag Berlin Heidelberg, 2003.

[2] K. Camacho, J. Burgos, and L. Combita, "Construction and modeling of a two-degree-of-freedom helicopter," in *Robotics Symposium and Latin American Robotics Symposium (SBR-LARS), 2012 Brazilian*, Oct 2012, pp. 150–155.

[3] Y. Watanabe, N. Katsurayama, I. Takami, and G. Chen, "Robust lq control with adaptive law for mimo descriptor system," in *9th Asian Control Conference (ASCC)*, June 2013, pp. 1–6.

[4] G.-R. Yu, "Robust-optimal control of a nonlinear two degree-of-freedom helicopter," *13th International Conference on Computer and Information Science (ICIS)*, pp. 744–749, 2007.

[5] Quanser, *Quanser 2-DOF Helicopter - Laboratory Manual*, 2nd ed., Quanser Inc., 2011.

[6] M. Guarnizo, R. Trujillo, and M. Guacaneme, "Modeling and control of a two dof helicopter using a robust control design based on dk iteration," in *IECON 2010 - 36th Annual Conference on IEEE Industrial Electronics Society*, Nov 2010, pp. 162–167.

[7] K. Ogata, *Modern Control Engineering*, 4th ed. Prentice Hall PTR, 2001.

[8] C. L. Phillips and R. D. Harbor, *Feedback Control Systems*, 4th ed. Prentice-Hall, Inc., 2000.